JACS
JOURNAL OF THE AMERICAN CHEMICAL SOCIETY
Article
pubs.acs.org/JACS

Self-Sorting of Foreign Proteins in a Bacterial Nanocompartment

W. Frederik Rurup,[†] Joost Snijder,[‡,§] Melissa S. T. Koay,*[,†] Albert J. R. Heck,[‡,§] and Jeroen J. L. M. Cornelissen[†]

[†]Laboratory for Biomolecular Nanotechnology, MESA+ Institute for Nanotechnology, University of Twente, P.O. Box 217, 7500 AE Enschede, The Netherlands

[‡]Biomolecular Mass Spectrometry and Proteomics, Bijvoet Center for Biomolecular Research and Utrecht Institute for Pharmaceutical Sciences, Utrecht University, Padualaan 8, 3584 CH Utrecht, The Netherlands

[§]Netherlands Proteomics Centre, Padualaan 8, 3584 CH Utrecht, The Netherlands

Supporting Information

ABSTRACT: Nature uses bottom-up approaches for the controlled assembly of highly ordered hierarchical structures with defined functionality, such as organelles, molecular motors, and transmembrane pumps. The field of bionanotechnology draws inspiration from nature by utilizing biomolecular building blocks such as DNA, proteins, and lipids, for the (self-) assembly of new structures for applications in biomedicine, optics, or electronics. Among the toolbox of available building blocks, proteins that form cage-like structures, such as viruses and virus-like particles, have been of particular interest since they form highly symmetrical assemblies and can be readily modified genetically or chemically both on the outer or inner surface. Bacterial encapsulins are a class of *nonviral* protein cages that self-assemble *in vivo* into stable icosahedral structures. Using teal fluorescent proteins (TFP) engineered with a specific native C-terminal docking sequence, we report the molecular self-sorting and selective packaging of TFP cargo into bacterial encapsulins during *in vivo* assembly. Using native mass spectrometry techniques, we show that loading of either monomeric or dimeric TFP cargo occurs with unprecedented high fidelity and exceptional loading accuracy. Such self-assembling systems equipped with self-sorting capabilities would open up exciting opportunities in nanotechnology, for example, as artificial (molecular storage or detoxification) organelles or as artificial cell factories for *in situ* biocatalysis.

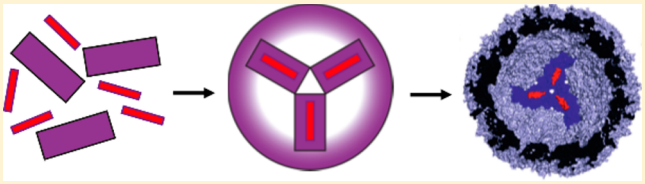

INTRODUCTION

Nature assembles small building blocks into highly sophisticated architectures such as DNA helices, viruses, membrane pumps, and organelles. Hierarchical assemblies that mimic their complexity have been of increasing interest for applications in nanotechnology and synthetic biology. For example, icosahedral virus-like structures have been shown to be highly useful for the encapsulation of a range of functional materials (i.e., proteins, polymers, nanoparticles, and inorganic complexes) for potential applications in nanomedicine, nanoelectronics, biomedical imaging, and catalysis.[1] In recent years, the library of engineered (synthetic and biological) assemblies has expanded tremendously, and there is now a growing trend to engineer inherently interacting proteins that can spontaneously self-assemble *in vitro* into complex structures.[2] In the reported cases, encapsulation of functional cargo is controlled by either creating fusion proteins or by introducing favorable electrostatic, hydrogen bonding, or hydrophobic interactions between the functional cargo and the protein scaffold.[3] However, in nature, this entire cargo loading and self-assembly process occurs in the crowded environment of the cell, yet does so with extremely high efficiency, and in the presence of multiple competitors. This high fidelity selectivity and affinity observed in biological systems is often termed *self-sorting*, the ability to identify self (desired cargo) from nonself (undesired cargo), and is extremely challenging to engineer using current methodologies.[4]

Bacterial encapsulins are the smallest member of an emerging class of protein cages called bacterial microcompartments, which also include the carboxysomes and metabolosomes.[2,5] Bacterial microcompartments act as simple protein-based organelles by confining enzymes and substrates within the confines of the protein cage. However, unlike carboxysomes and metabolosomes, which play important roles in confining metabolic pathways that involve the formation of toxic or volatile intermediates, bacterial encapsulins from *Brevibacterium linens* and *Thermatoga maritima* contain either a dye-decolorizing peroxidase (DyP) or a ferritin-like protein (Flp), both of which are involved in oxidative stress.[6] For the case of *B. linens* encapsulins, the dye-decolorizing peroxidase is assembled as a trimer of dimers inside the internal cavity (i.e., a 1:10 ratio of cargo per encapsulin monomer), whereas *T. maritima* reportedly packages a pentamer of Flp dimers (Figure 1). Bacterial encapsulins are composed of 60 identical protein subunits that form Caspar–Klug type $T = 1$ assemblies of approximately 24 nm in diameter.[6,7] Although morphologically similar to small icosahedral plant-based viruses, both structural

Received: October 24, 2013
Published: February 14, 2014

   dx.doi.org/10.1021/ja410891c | J. Am. Chem. Soc. 2014, 136, 3828–3832

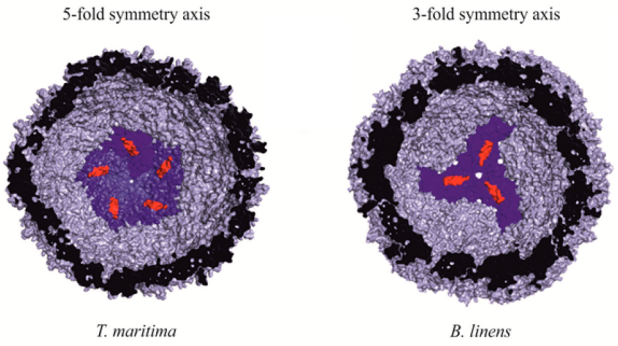

Figure 1. Interior view of the (a) *T. maritima* and (b) *B. linens* bacterial encapsulins, with their corresponding pentamers and trimers (shown in blue). The specific C-terminal docking sequence (shown in red) promotes the selective packaging of molecular cargo during *in vivo* self-assembly.

and gene homology studies suggest that encapsulins are of nonviral origin, due to the absence of any genes of viral origin within the vicinity of the encapsulin gene.[6,7]

Unlike viruses such as Cowpea Chlorotic Mottle Virus (CCMV), which undergo *in vitro* pH-driven reversible assembly/disassembly, bacterial encapsulins are highly pH- and temperature-stable and are assembled entirely *in vivo*. Importantly, cargo loading in bacterial encapsulins is significantly different from that of virus-based assemblies. Whereas CCMV capsid proteins contain a highly positively charged N-terminus that acts as an electrostatic template for the encapsulation of (negatively charged) genetic DNA/RNA cargo, molecular reconstruction studies revealed that encapsulins contain a highly conserved C-terminal docking sequence composed of 30−40 amino acids.[6,7] This docking sequence interacts with a hydrophobic binding pocket within the inner wall of the encapsulin and is thought to infer the precise orientation and alignment of the native DyP cargo along the interior of the *B. linens* encapsulin. Despite the variation in length, this C-terminal extension consists of a high content of alanine, glycine, and proline residues, followed by a conserved anchor sequence. We anticipated that this docking sequence could be used to direct and orient non-native cargo inside the bacterial encapsulin during *in vivo* assembly. Using teal fluorescent protein (TFP), we show that engineering the docking sequence at the C-terminus of non-native protein cargo promotes selective packaging in the bacterial encapsulin of *B. linens* with high fidelity and exceptional loading accuracy.

RESULTS AND DISCUSSION

To study the self-sorting properties and selective packaging of the *B. linens* encapsulin, we genetically engineered the docking sequence to the C-terminus of TFP and determined the loading efficiency of fluorescent proteins per encapsulin assembly. To do so, we replaced the gene encoding for the native DyP (immediately preceding the gene encoding for the C-terminal docking sequence) with that of TFP. TFP was chosen as the foreign cargo owing to its ease of detection, superior brightness, and pH- and photostability.[8] Furthermore, point mutations can easily be introduced onto the surface of TFP to promote dimerization, thereby allowing us to study the effects of multivalency on cargo loading (i.e., whether dimerization improves cargo loading efficiency inside the encapsulin). To show the cargo selectivity and self-sorting nature of cargo

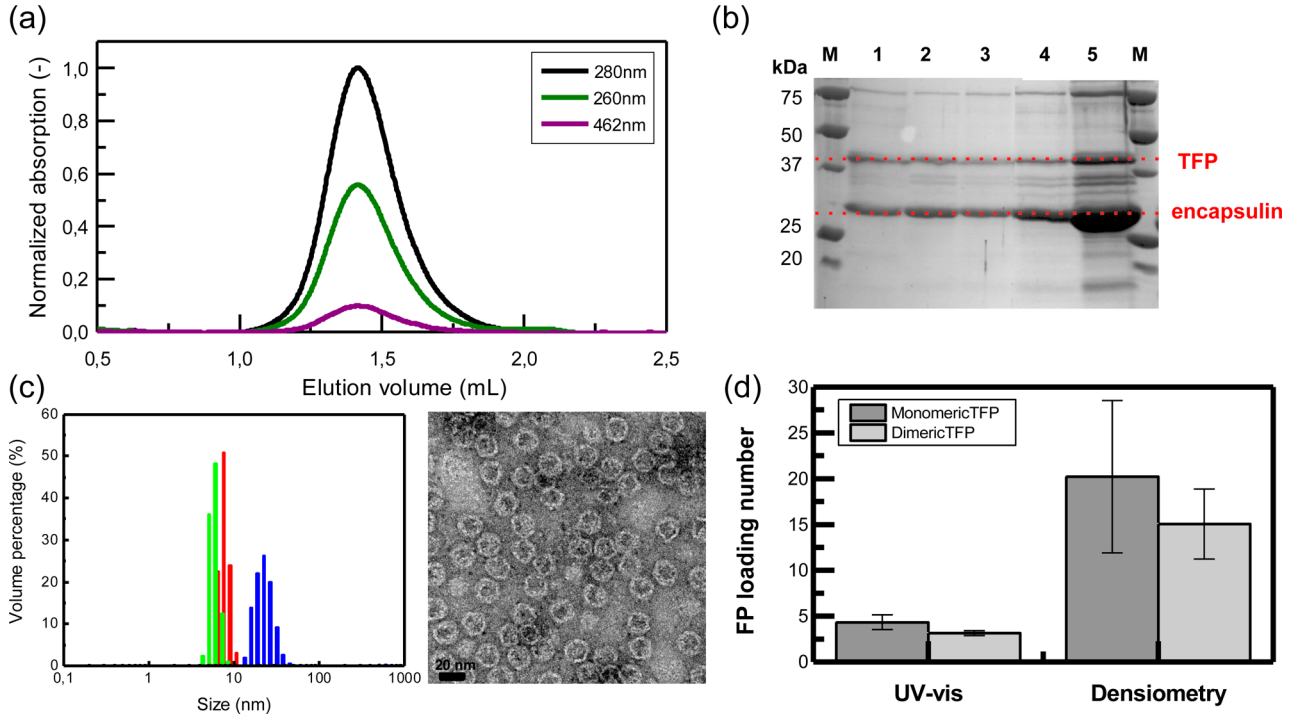

Figure 2. (a) Purification by size exclusion chromatography shows the coelution of the *B. linens* encapsulin (λ = 280, 260 nm) and mTFP (λ = 462 nm) at 1.3 mL. (b) Quantitative SDS-PAGE densiometry analysis of purified mTFP-filled and dTFP-filled encapsulins showing consistent TFP to encapsulin ratios. (c) Dynamic light scattering (DLS) of nonencapsulated mTFP (green), nonencapsulated dTFP (red), and intact encapsulins (blue) and transmission electron microscopy (TEM) confirm the size (diameter 24 nm) and morphology of the purified mTFP loaded bacterial encapsulins. (d) Comparison of the various techniques used for the quantification of mTFP and dTFP in encapsulins.

dx.doi.org/10.1021/ja410891c | J. Am. Chem. Soc. 2014, 136, 3828−3832

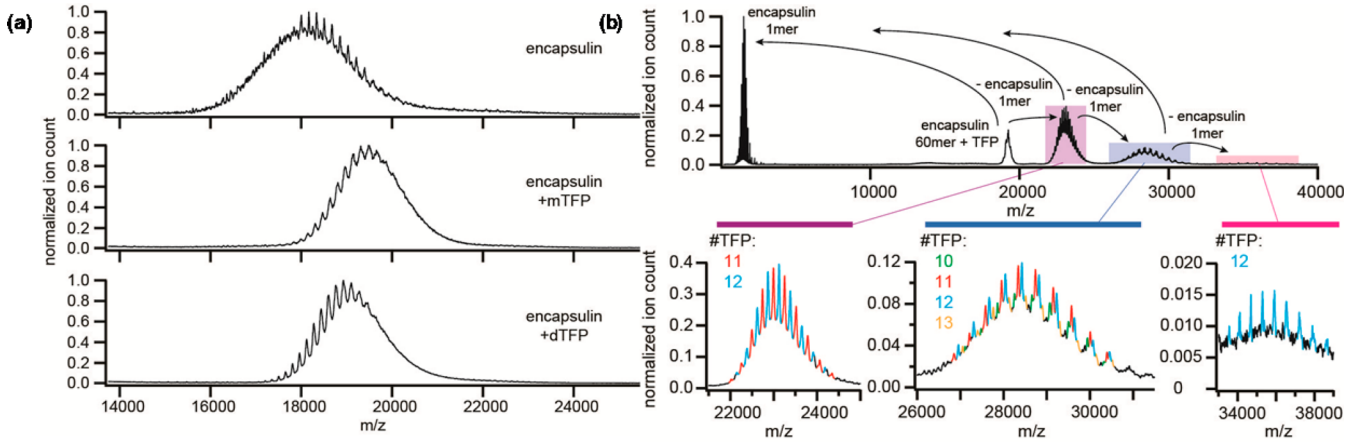

Figure 3. (a) Native mass spectrometry of the empty, mTFP filled, and dTFP filled *B. linens* bacterial encapsulins. (b) Collision-induced dissociated tandem mass spectrometry of the *B. linens* bacterial encapsulin. The stepwise dissociation products confirmed the presence of dTFP in *B. linens* bacterial encapsulins.

loading in encapsulins, we also expressed empty encapsulins lacking the C-terminal docking sequence (and hence, any targeted cargo).

Since assembly of the encapsulins occurs entirely *in vivo*, all encapsulins were purified as preassembled intact protein cages. Similar to virus-based assemblies, purification could be achieved by differential centrifugation techniques. Further purification of the TFP containing encapsulins was performed by size exclusion chromatography, monitoring at λ = 462, 280, and 260 nm, which correspond to both TFP (λ = 462, 280 nm) and bacterial encapsulins (λ = 280, 260 nm), respectively. The overlapping elution peak positions strongly implied that TFP was successfully coassembled with the encapsulins (Figure 2a). In addition, all encapsulins confirmed a single band eluting at 1.4 mL, which is reminiscent of icosahedral virus-like assemblies of similar morphology and apparent size.[3d] TFP and encapsulin coassembly was further confirmed by denaturing SDS-PAGE analysis, which revealed the presence of both TFP bearing the C-terminal docking sequence (34.7 kDa) and the encapsulin monomer (28.6 kDa) in the purified fractions (Figure 2b). Particle size analysis by dynamic light scattering (DLS) and transmission electron microscopy (TEM) showed highly monodisperse particles with the expected diameter of 24 nm and the correct morphology of intact encapsulins (Figure 2c). As a control experiment, the empty *B. linens* encapsulin (lacking the C-terminal docking sequence) failed to show any absorbance at λ = 462 nm, thereby confirming that no TFP is inadvertently coexpressed in the cell. Denaturing SDS-PAGE analysis of empty encapsulins revealed a single protein band corresponding to the encapsulin monomer, confirming that no other unwanted proteins are packaged inside the encapsulin (Supporting Information Figure S2). The elution of empty encapsulins at 1.4 mL also confirms that the C-terminal docking sequence is not essential for encapsulin assembly itself, but is associated with selective cargo loading. This is also consistent with previous studies, which have shown that DyP species lacking the C-terminal docking sequence are not packaged inside the encapsulin despite their high expression levels.[6,7] In the past, we reported that the average loading of fluorescent cargo in CCMV based assemblies can be determined by correlating the specific absorbance of the fluorescent protein (λ = 462 nm) and the virus capsid monomer (λ = 280 nm).[3d] On the basis of the calculated extinction coefficient of 64 000 M^{-1} cm^{-1} for TFP at 462 nm,[9] we calculated a loading of only 4.3 ± 0.8 mTFP (monomeric teal fluorescent protein) within the *B. linens* encapsulin. (All cargo quantification experiments were performed at least five times.)

Due to the unexpected low loading number, we attempted to improve the loading efficiency. To do so, we re-engineered TFP at the monomer interface to restore its natural homodimerization. In the past, we have shown that restoring five hydrophobic mutations (D144E, A145P, R149I, K162S, and K164S) promotes TFP dimerization (dTFP, dimeric teal fluorescent protein) and that the loading efficiency into the capsid of CCMV is improved.[9] Interestingly, introducing the same mutations here did not improve the loading efficiencies for mTFP (4.3 ± 0.8 mTFPs) compared to dTFP (3.1 ± 0.3 dTFP monomers), despite both DNA sequencing and dynamic light scattering (DLS) confirming that TFP dimerization had been restored (Supporting Information Figure S1 and Figure 2d, respectively). However, it should be noted that TFP quantification by UV−vis spectroscopy relies heavily on the correct conformation of the chromophore. In our case, we cannot eliminate the possibility that the C-terminal docking sequence (or packaging in the encapsulin itself) does not affect or distort chromophore formation, and hence perturb accurate quantification.[8,10]

To further investigate this discrepancy, the relative intensity of the protein bands corresponding to TFP (bearing the C-terminal docking sequence, 34.7 kDa) and *B. linens* encapsulin (monomer, 28.6 kDa) were compared and quantified on the basis of quantitative SDS-PAGE analysis (Figure 2b). Assuming each encapsulin is composed of 60 encapsulin monomers, an average ratio of 20.2 ± 8.3 mTFPs and 15.1 ± 3.8 dTFP monomers was quantified. Due to the large difference between the two techniques, we sought a third and more accurate technique. Therefore, we employed native mass spectrometry to determine the number of TFP (monomers) present. Native mass spectrometry is a highly sensitive and extremely precise technique that has been used to determine the exact mass of intact virus-based assemblies.[11] Empty and TFP filled encapsulins show signals centered at 18 000 and 19 000 m/z, respectively, with extensive overlap between peaks (Figure 3a). The peak width suggests heterogeneity among the encapsulin assemblies; however, on the basis of the expected masses for

dx.doi.org/10.1021/ja410891c | J. Am. Chem. Soc. 2014, 136, 3828−3832

TFP bearing the C-terminal docking sequence (34.7 kDa) and the encapsulin monomer (28.6 kDa), the calculated masses correlated to an average of 12.2 ± 2.0 mTFP and 6.2 ± 0.9 dTFPs (12.4 ± 1.9 monomers) per encapsulin. Detailed quantitative analysis was performed using collision-induced dissociation tandem MS (CID-MS2), which allows for a more accurate mass assignment since a specific region of interest is selected for collision-induced dissociation and subsequently analyzed in the time-of-flight mass analyzer. CID-MS2 revealed additional peaks that could be assigned to the stepwise dissociation of encapsulin, i.e., loss of single monomeric encapsulin protein (Figure 3b). While the intact encapsulin showed only a single series of resolved charge states, two series of peaks could be resolved in the first dissociation product (loss of one subunit), four series of peaks in the second product, and one series in the third product.

Interestingly, the mass distributions corresponded to 9.0, 10.0, and 11.0 mTFPs and 10.0, 11.0, 12.0, and 13.0 dTFP monomers per encapsulin, respectively. The presence of an odd number of dTFP monomers suggests that dimerization is perturbed during *in vivo* loading and/or packaging into bacterial encapsulins, despite both DLS and DNA sequencing results which confirmed TFP dimerization (Figure 2b). Nonetheless, the average MS1 data and the CID-MS2 data showed no significant difference in loading efficiency between mTFP and dTFP, suggesting that the driving force for cargo docking and encapsulation could be much greater than cargo dimerization interactions.

In the native encapsulin of *B. linens,* a trimer of DyP dimers (100 Å in each direction) occupies the entire inner cavity of the encapsulin (220 Å diameter). By comparison, a homologous encapsulin from *Thermatoga maritima* was shown to contain a pentamer of dimers of ferritin-like proteins (Flp) within its inner cavity.[6] This difference in loading number is thought to be due to the relative size of the cargo, whereby the ferritin-like protein (Flp) is much smaller (globally) compared to the dye-decolorizing peroxidase (DyP). In the case of the small β-barrel mTFP and dTFP, we show that an average of 12 TFP cargo molecules can be packaged with high fidelity and exceptional loading accuracy. Interestingly, these numbers correlate extremely well with the number of pentamers required for encapsulin assembly (12 pentamers and average of 12 cargo), which may suggest a highly concerted assembly process in which each fluorescent protein is docked at each pentamer. It should also be noted that we consistently observed over-expression of TFP cargo compared to encapsulin expression levels. This overexpression of TFP and the fact that any excess TFP is not packaged in encapsulins could indicate that the greater cargo cannot be accommodated within the inner cavity, which has also been reported for the native DyP enzyme.[6]

The high loading accuracy, combined with the monodispersity, stability, and robust nature of bacterial encapsulins, makes them highly promising candidates for future applications in nanotechnology. While there are examples reported of designed protein cages that promote cargo packaging during *in vivo* self-assembly,[13] bacterial encapsulins are the first example of a nonviral protein cage which contains a *naturally encoded* self-sorting peptidic sequence. Moreover, since the entire packaging and assembly occurs *in vivo* in the presence of ≥2600 cytosolic *E. coli* proteins,[12] this work demonstrates the *self-sorting* nature of encapsulins by the *selective* packaging of cargo bearing the C-terminal docking sequence. Such self-assembling systems equipped with self-sorting capabilities would open up a new realm of exciting opportunities in nanotechnology, as artificial organelles or as cell factories for *in situ* biocatalysis.

EXPERIMENTAL SECTION

Molecular Cloning of *B. linens* Encapsulin. The pET21a-based plasmid vector encoding the two-gene operon of *Brevibacterium linens* M18 encapsulin and its native cargo protein dye-decolorizing peroxidase (DyP) was a kind gift from Sutter et al.[7] Site-directed mutagenesis was performed using standard QuikChange site directed mutagenesis techniques (Stratagene) to introduce a unique *Bam*HI site at the 3′-end of the DyP gene. Using *Bam*HI and *XbaI* double enzyme restriction digestion, the original DyP gene was replaced with monomeric teal fluorescent protein (mTFP) bearing the C-terminal docking peptide, for recombinant coexpression and *in vivo* packaging of monomeric TFP into the bacterial encapsulin of *B. linens*. On the basis of the same cloning procedure as described for mTFP, the original DyP gene was replaced with dimeric teal fluorescent protein (dTFP), bearing the C-terminal docking peptide, for recombinant coexpression and *in vivo* packaging of dimeric TFP into the encapsulin. All genetically engineered vector constructs were confirmed by DNA sequencing (MWG Eurofins, Germany).

Encapsulin Expression and Purification. Recombinant expression was performed using *E. coli* Rosetta (DE3) as an expression host. The cells were grown to an o.d. (600 nm) of 0.6 before inducing with isopropyl-β-D-1-thiogalactopyranoside overnight at 22 °C. As a comparative control, empty *B. linens* encapsulin (lacking the C-terminal docking sequence) was also expressed recombinantly in *E. coli*. The harvested bacterial cells were lysed in 20 mM Tris-Cl buffer, 150 mM NH_4Cl, 20 mM $MgCl_2$, and 1 mM β-mercaptoethanol (pH 7.5) in the presence of DNase and RNase. The cell debris was removed by ultracentrifugation (162 000 × *g*, 15 min), and the cell lysate containing intact encapsulins was purified by 38% sucrose cushion (162 000 × *g*, 17 h). The pellet containing crude *B. linens* encapsulins was carefully resuspended in 20 mM Tris-Cl buffer, 150 mM NH_4Cl, 20 mM $MgCl_2$, and 1 mM β-mercaptoethanol (pH 7.5) and purified by 10−50% sucrose gradient (162,000 × *g*, 17 h). The fractions containing encapsulins were collected and further purified by fast protein liquid chromatography (FPLC) using a Superose 6 10/100 GL (GE Healthcare) preparative column, monitoring at λ = 260, 280, and 462 nm for empty, mTFP, and dTFP loaded encapsulins. The elution profiles for both the mTFP and dTFP loaded encapsulins confirmed the coelution of fluorescent proteins with the assembled encapsulins.

UV−Vis Spectrometry. All measurements were performed on a Perkin-Elmer Lambda 850 spectrometer. Standard quartz cuvettes with a 1 cm path length were used. The slit widths are optimized to achieve the best signal-to-noise ratio.

SDS-PAGE Densitometry. Standard SDS-PAGE was performed with 12% polyacrylamide gels using PeqLab systems. Bio-Safe Coomassie (Bio-Rad laboratories, Inc.) was used to visualize the protein bands. SDS-PAGE densitometry analyses were performed using ImageJ software version 1.46.

Transmission Electron Microscopy. TEM measurements were performed on a Philips CM 30 analytical FEG-TEM operated at an acceleration voltage of 300 kV. Samples were prepared by placing 5 μL of the samples on Formvar carbon-coated copper grids (Electron Microscopy Sciences). The sample was incubated on the grid for 5 min, before the excess buffer was removed with filter paper. Samples were negatively stained by applying 5 μL uranyl acetate (1% w/v) onto the grid and incubating for 1 min. The excess stain was removed, and the samples were left to dry overnight before imaging.

Mass Spectrometry. All samples were prepared for mass spectrometry by repeated dilution and concentration to exchange the buffer to 100 mM ammonium acetate (pH 6.8−7.0), using Vivaspin 500 10K MWCO centrifugal filter units. Aliquots of 1−2 μL were loaded into gold-coated borosilicate capillaries, prepared in−house, for nanoelectrospray ionization. Samples were analyzed on a modified QToF II instrument optimized for high-mass protein analysis.[11] The instrument operates at elevated pressure in the source

dx.doi.org/10.1021/ja410891c | J. Am. Chem. Soc. 2014, 136, 3828−3832

region and hexapole ion guide, which results in collisional cooling of the ions and improves transmission. The measurements were performed with xenon as collision gas. The source conditions for the encapsulin were as follows: capillary 1300−1500 V, cone 160 V, extraction cone 0 V, and 10 mbar backing pressure. The pressure in the collision cell was 2×10^{-2} mbar.

Quantification of Fluorescent Cargo. Quantitative SDS-PAGE analysis was performed to correlate the average ratio of monomeric or dimeric TFP per encapsulin monomer, using ImageJ software (version 1.46) gel analyzer tool (to analyze the intensity ratios of the 34.7 kDa TFP band to the 28.6 kDa *B. linens* band). On the basis of the relative protein band intensities for TFP (bearing the C-terminal docking sequence; expected mass 34.7 kDa) and the *B. linens* encapsulin monomer (expected mass 28.6 kDa), an average number of TFPs per encapsulin could be determined. All quantification experiments were performed in quintuplicate.

■ ASSOCIATED CONTENT

Ⓢ Supporting Information

DNA sequence alignment of mTFP and dTFP. Characterization by SDS-PAGE and TEM of DyP containing encapsulins and empty enacpsulins. This material is available free of charge via the Internet at http://pubs.acs.org

■ AUTHOR INFORMATION

Corresponding Author

m.s.t.koay@utwente.nl

Author Contributions

All authors have given approval to the final version of the manuscript.

Notes

The authors declare no competing financial interest.

■ ACKNOWLEDGMENTS

The authors acknowledge financial support by the Chemical Council of The Netherlands National Science Foundation (NWO-CW), the European Science Foundation (ESF), and The Netherlands Royal Academy for Arts and Sciences (KNAW). We are grateful to Prof. Nenad Ban and Dr. Markus Sutter for fruitful discussions and the kind donation of plasmids.

■ REFERENCES

(1) (a) Douglas, T.; Young, M. *Science* **2006**, *312*, 873. (b) Fischlechner, M.; Donath, E. *Angew. Chem.* **2007**, *46*, 3184. (c) Kramer, R. M.; Li, C.; Carter, D. C.; Stone, M. O.; Naik, R. R. *J. Am. Chem. Soc.* **2004**, *126*, 13282. (d) Ma, Y.; Nolte, R. J.; Cornelissen, J. J. L. M. *Adv. Drug Delivery Rev.* **2012**, *64*, 811. (e) Rego, J. M.; Yi, H. In *Supramolecular Chemistry: From Molecules to Nanomaterials*; John Wiley & Sons, Ltd.: Hoboken, NJ, 2012. (f) Singh, P.; Gonzalez, M. J.; Manchester, M. *Drug Dev. Res.* **2006**, *67*, 23. (g) Young, M.; Debbie, W.; Uchida, M.; Douglas, T. *Annu. Rev. Phytopathol.* **2008**, *46*, 361.

(2) Tanaka, S.; Sawaya, M. R.; Yeates, T. O. *Science* **2010**, *327*, 81.

(3) (a) Comellas-Aragones, M.; Engelkamp, H.; Claessen, V. I.; Sommerdijk, N. A.; Rowan, A. E.; Christianen, P. C.; Maan, J. C.; Verduin, B. J.; Cornelissen, J. J. L. M.; Nolte, R. J. M. *Nat. Nanotechnol.* **2007**, *2*, 635. (b) Fiedler, J. D.; Brown, S. D.; Lau, J. L.; Finn, M. G. *Angew. Chem.* **2010**, *49*, 9648. (c) Glasgow, J. E.; Capehart, S. L.; Francis, M. B.; Tullman-Ercek, D. *ACS Nano* **2012**, *6*, 8658. (d) Minten, I. J.; Hendriks, L. J. A.; Nolte, R. J. M.; Cornelissen, J. J. L. M. *J. Am. Chem. Soc.* **2009**, *131*, 17771. (e) O'Neil, A.; Prevelige, P. E.; Basu, G.; Douglas, T. *Biomacromolecules* **2012**, *13*, 3902. (f) O'Neil, A.; Reichhardt, C.; Johnson, B.; Prevelige, P. E.; Douglas, T. *Angew. Chem.* **2011**, *50*, 7425. (g) Patterson, D. P.; Prevelige, P. E.; Douglas, T. *ACS Nano* **2012**, *6*, 5000.

(4) (a) Safont-Sempere, M. M.; Fernández, G.; Würthner, F. *Chem. Rev.* **2011**, *111*, 5784. (b) Whitesides, G.; Mathias, J.; Seto, C. *Science* **1991**, *254*, 1312.

(5) (a) Cannon, G.; Bradburne, C.; Aldrich, H.; Baker, S.; Heinhorst, S.; Shively, J. *Appl. Environ. Microbiol.* **2001**, *67*, 5351. (b) Frank, S.; Lawrence, A. D.; Prentice, M. B.; Warren, M. J. *J. Biotechnol.* **2013**, *163*, 273. (c) Kerfeld, C. A.; Heinhorst, S.; Cannon, G. C. *Annu. Rev. Microbiol.* **2010**, *64*, 391. (d) Tanaka, S.; Kerfeld, C. A.; Sawaya, M. R.; Cai, F.; Heinhorst, S.; Cannon, G. C.; Yeates, T. O. *Science* **2008**, *319*, 1083.

(6) Sutter, M.; Boehringer, D.; Gutmann, S.; Gunther, S.; Prangishvili, D.; Loessner, M. J.; Stetter, K. O.; Weber-Ban, E.; Ban, N. *Nat. Struct. Mol. Biol.* **2008**, *15*, 939.

(7) Sutter, M. Ph.D. Dissertation, ETH Zurich, 2008.

(8) Ai, H.-w.; Henderson, J. N.; Remington, S. J.; Campbell, R. E. *Biochem. J.* **2006**, *400*, 531.

(9) Rurup, W. F.; Verbij, F.; Koay, M. S. T.; Blum, C.; Subramaniam, V.; Cornelissen, J. J. L. M. *Biomacromolecules* **2014**, *15*, 558.

(10) Topol, I.; Collins, J.; Nemukhin, A. *Biophys. Chem.* **2010**, *149*, 78.

(11) (a) Snijder, J.; Rose, R. J.; Veesler, D.; Johnson, J. E.; Heck, A. J. R. *Angew. Chem.* **2013**, *52*, 4020. (b) Uetrecht, C.; Barbu, I. M.; Shoemaker, G. K.; van Duijn, E.; Heck, A. J. R. *Nat. Chem.* **2011**, *3*, 126. (c) Van Den Heuvel, R. H. H.; van Duijn, E.; Mazon, H.; Synowsky, S. A.; Lorenzen, K.; Versluis, C.; Brouns, S. J. J.; Langridge, D.; van der Oost, J.; Hoyes, J.; Heck, A. J. R. *Anal. Chem.* **2011**, *78*, 7473.

(12) Ishihama, Y.; Schmidt, T.; Rappsilber, J.; Mann, M.; Hartl, F.; Kerner, M.; Frishman, D. *BMC Genomics* **2008**, *9*, 1.

(13) Worsdorfer, B.; Woycechowsky, K. J.; Hilvert, D. *Science* **2011**, *331*, 589.